SIMULATION OF THE SIGNAL PROCESSING FOR THE NEW INTERACTION REGION BPMs OF THE HIGH LUMONSITY LHC

D. R. Bett*, University of Oxford, UK

M. Wendt, M. Krupa, A. Boccardi, CERN, Geneva, Switzerland

Abstract

New stripline beam position monitors (BPMs) will be installed at the Interaction Regions of the ATLAS and CMS experiments as part of the High-Luminosity upgrade to the LHC. These BPMs will be located in sections of the beamline where the two counter-propagating proton beams co-exist within a single pipe, such that the signal observed on each output port is a combination of the signals generated by each beam. The use of the BPMs as the input for a possible luminosity feedback system places a demanding requirement on the long-term accuracy of the BPMs. Accurate measurement of the position of each beam requires a method for isolating the individual beam signals. A simulation framework has been developed covering all stages of the measurement process, from generation of the signals expected for beams of a given intensity and orbit through to digitization, and has been used to evaluate several candidate methods for extracting the position of each beam in the presence of the unwanted signal from the other.

INTRODUCTION

The High Luminosity LHC is an upgrade of the LHC with a target luminosity five times larger than the current nominal value of 10^{34} cm^{-2}s^{-1}. As part of this upgrade, the beam position monitors (BPMs) in interaction region (IR) 1 and 5 will be replaced, corresponding to the vicinity of the ATLAS and CMS detectors respectively.

The layout of the right side of IR1 and IR5 is illustrated in Fig. 1. Far from the interaction point (IP) the proton beams exist in their own individual pipes and the BPMs need only measure the position of the one beam. Close to the IP, the two beams travel within the same pipe and the BPMs in that region are required to measure the position of both beams. Six new octagonal stripline BPMs of two different types will be installed either side of each of the two IPs, with the BPM closest to the IP being of type A and the remainder of type B. The two types have slightly different apertures and will be installed with different orientations of the electrodes; type A BPMs will have the electrodes oriented at 0° and 90° in the lab frame and the type B BPMs will be rotated by 45° due to the tungsten shielding at those locations. The longitudinal location of each BPM, s, determines the difference in arrival time of the two beams, Δt (Table 1).

BPM MODEL

The CST Microwave Studio [1] model of the type A BPM is shown in Fig. 2. I_1 and I_2 represent beams entering the

---

* douglas.bett@physics.ox.ac.uk

Table 1: BPM distance from the IP (s) and difference in the arrival time of the two beams (Δt).

BPM Type	s [m]	Δt [ns]
A	21.853	3.92
B	33.073	3.92
B	43.858	6.82
B	54.643	9.72
B	65.743	10.52
B	73.697	7.36

BPM from opposite directions and V_1 to V_8 the signals observed at each end of the four striplines designated right (R), top (T), left (L) and bottom (B). Stripline BPMs are highly directive [2]; in the ideal case, there is perfect cancellation at the downstream ports between the signal induced in the direction of the beam as the beam enters the BPM, and the signal induced as the beam exits the BPM. The resulting bipolar signal is therefore only observed at the upstream port. This allows such a BPM to be used to distinguish the signal generated by beams travelling in opposite directions.

In practice the cancellation is not total and a small amount of signal is observed at the downstream end, combining with main signal from the opposite beam. Figure 3 shows the voltages calculated at each end of each stripline when a simulated beam with the indicated current profile travels along the BPM axis. The first beam to arrive is designated "beam 1" and induces a large ("coupled") signal at upstream ports 1-4 and a much smaller ("isolated") signal at downstream ports 5-8, while the reverse is true for "beam 2" which enters the other end of the BPM after time Δt. Each beam distorts the signals that will be used to measure the position of the other beam, and this distortion must be taken into account in order to obtain accurate measurements of the position of each individual beam.

SIMULATION

The numerical computation software GNU Octave [3] was used to simulate the process of obtaining beam position measurements from the stripline signals. The CST predictions of the signals induced at each end of the stripline are scaled according to the position and charge of each beam and the signals from beam 2 are delayed as appropriate in order to form the set of stripline waveforms V_1 to V_8. As the BPMs are located in a very high-radiation environment, long (> 100 m) cables will be used to transport the signals to a digital processor able to operate at a sample frequency of ~ 4 GHz. Given the pulses themselves are only a few
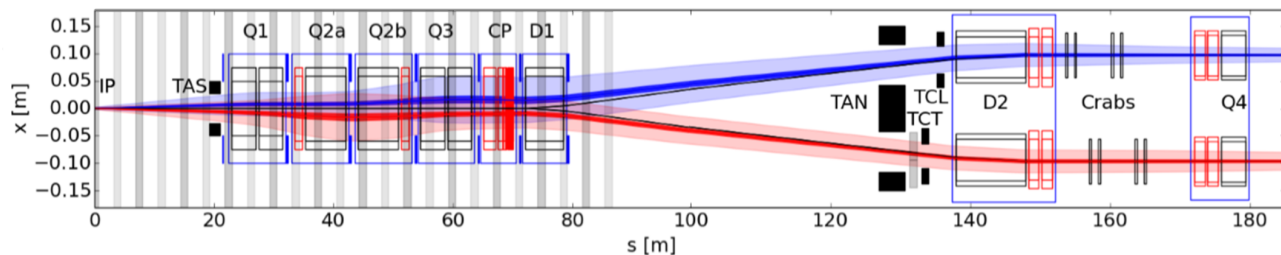
Figure 1: Beam optics in the interaction regions [4]. The dark blue and red strips correspond to the 2σ envelope of the beams and the vertical blue bars either side indicate the locations of the BPMs.
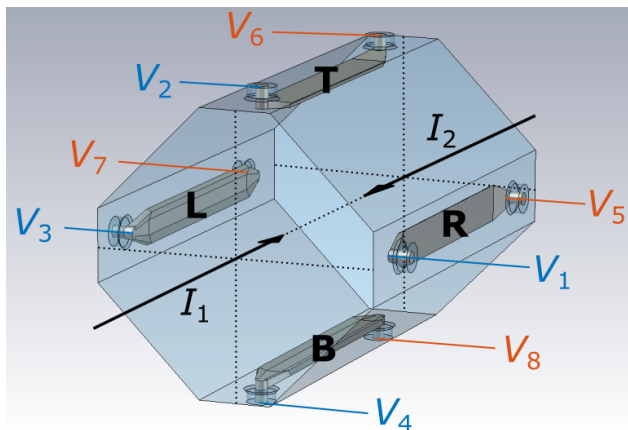

Figure 2: 3D model of the type A BPM in CST Microwave Studio with annotation indicating the beam inputs I_1 and I_2 and the stripline outputs V_1 through V_8.

Table 2: Simulation Parameters

Property	Value
(x_1, y_1)	$(0.75, -6.45)$ mm
(x_2, y_2)	$(-0.75, 6.15)$ mm
Δt	3.92 ns
Beam 1 population	2.3×10^{11} charges
Beam 2 population	2.3×10^{10} charges
Bunch profile	Gaussian, FWHM = 0.95 ns (both)
Cable attenuation	7.19 dB/100 m @ 1 GHz
Cable velocity	$0.88c$
Cable length	100 m
Cut-off frequency	273 MHz

tizer. The situation depicted is an extreme case where the charge of beam 1 is ten times higher than that of beam 2, but it serves to illustrate that a small signal from beam 1 is followed $\Delta t = 3.92$ ns later by a larger signal from beam 2. Table 2 lists the values used for the relevant simulation properties; the beam orbits correspond to the pre-squeeze orbits of the beams at the IR1 type A BPM.
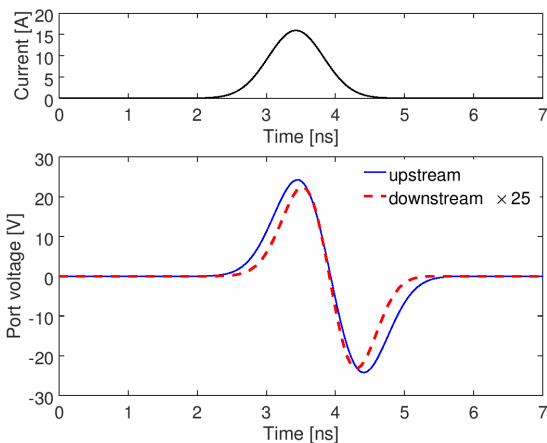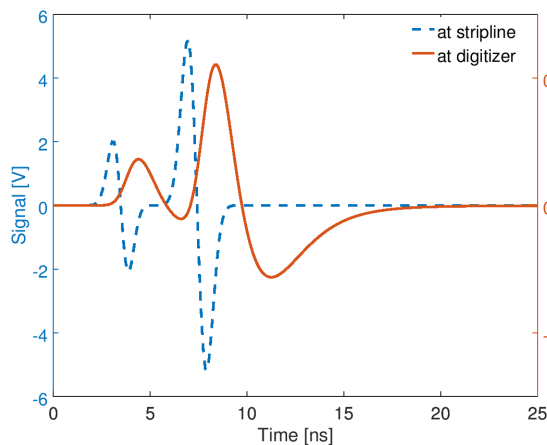

Figure 3: Input beam current profile (top) and voltage induced at the upstream end (solid) and the downstream end (dashed and magnified x25).

Figure 4: Appearance of V_5 at the stripline (dashed; left axis) and after low pass filtering at the digitizer (solid; right axis) for the simulation parameters given in Table 2.

nanoseconds long (Fig. 3), the 25 ns bunch spacing between HL-LHC bunches motivates the use of a low-pass filter to make more efficient use of the ADCs by stretching the signals in the time domain. As both ends of the stripline are monitored, a reflectionless filter was implemented [5]. Figure 4 shows how the port 5 (downstream) signals are expected to appear at the stripline itself and at the input to the digi-

Variable attenuators are also included in order to match the levels of the analogue stripline signals to the range of the digitizer. The digitization process itself is assumed to

be asynchronous with respect to the beam and to inject a realistic amount of random noise into the system based on measurements taken with a candidate digitizer. The digital waveforms are then ready to be processed in order to calculate the beam positions.

COMPENSATION

Several methods of compensating the waveforms to account for the signal from the other beam were considered. These included explicit sample-by-sample subtraction of a reference waveform (scaled according to the observed amplitude of the waveform from the other end of the stripline) and a frequency domain approach that assumed the response of the BPM and the other hardware could be measured well enough to be able to recover the image current induced by each beam on each stripline.

An ensemble of 2,760 pulses at the same position was generated by digitizing the set of eight stripline signals generated in the previous section at 12-bit resolution with a 4 GHz sample clock. The clock phase varied uniformly and 1.5 bits of randomly distributed noise was added to each sample. Each set of eight waveforms was then used to perform a position measurement and Fig. 5 shows the results with the "ideal" position that would be measured by the stripline subtracted (note that this position differs from the true position of the beam as the non-linearity of the BPM is not taken into account). The frequency domain method clearly performs the worst and, for the beam conditions outlined here, is in fact worse than not compensating at all, as the offset of the measured mean position is 25 μm compared to less than 3 μm for no compensation. Both the sample-by-sample and power methods reduce this offset to less than half a micron. The single-pass error is approximately 10 μm regardless of whether compensation is performed or not. Power compensation is thus the preferred method as it requires by far the smallest amount of digital processing power.
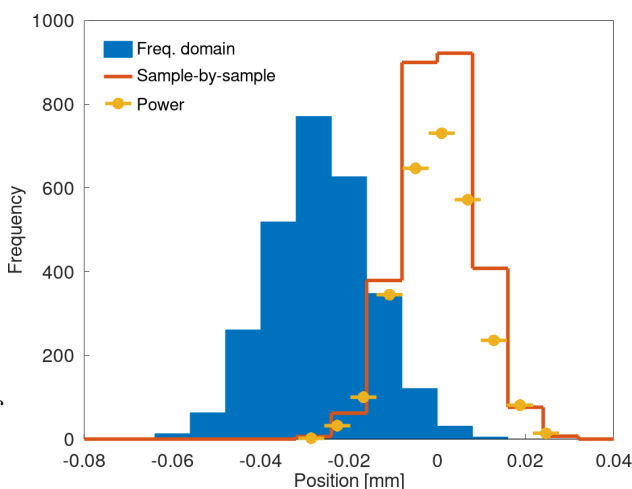

Figure 5: Histograms of the estimated horizontal position of beam 2 for several different methods of compensating for the other beam: frequency domain (solid), sample-by-sample (outline) and power (points).

Power Compensation Method

Consider the signal induced at the upstream end of the R stripline:

$$V_1 = \kappa_{1R} V_{1c} + \kappa_{2R} V_{2i} \qquad (1)$$

where:

- V_{1c} is the signal induced at the upstream end of each stripline by a reference beam 1 with some nominal intensity and bunch length that travels on axis.

- V_{2i} is the signal induced by a reference beam 2 which has the same intensity and bunch length as the reference beam 1 and likewise travels on axis.

- The κ scale factors set the amplitude of each term of the stripline signal according to the intensity of each beam and its position in the BPM. $\kappa_{ij} = \rho_{ij} \cdot q_i$, where q_i is the intensity of the actual beam i (expressed as a multiple of the intensity of the reference beam) and ρ_{ij} is the angle subtended by beam i on stripline j (expressed as a multiple of the angle subtended from the center of the BPM).

Taking the sum of the samples squared for both sides:

$$\sum V_1^2 = \kappa_{1R}^2 \sum V_{1c}^2 + 2\kappa_{1R}\kappa_{2R} \sum V_{1c} \cdot V_{2i} + \kappa_{2R}^2 \sum V_{2i}^2 \qquad (2)$$

Let $\sum V_i^2 = \psi_i$ and $\sum V_i \cdot V_j = \chi_{ij}$; then Eq. 2 can be rearranged so as to resemble a quadratic equation:

$$\kappa_{1R}^2 + 2\frac{\chi_{1c2i}}{\psi_{1c}}\kappa_{1R}\kappa_{2R} + \left(\frac{\psi_{2i}}{\psi_{1c}}\kappa_{2R}^2 - \frac{\psi_1}{\psi_{1c}}\right) = 0 \qquad (3)$$

By making the approximation $\kappa_{2R} \sim \sqrt{\frac{\psi_5}{\psi_{2c}}}$, the coefficients of this quadratic equation can be expressed solely in terms of a set of scalars that can be calculated in advance from the reference waveforms ($\psi_{1c}, \psi_{2i}, \chi_{1c2i}$) and a pair of scalars that must be calculated in real time from the measured waveforms (ψ_1, ψ_5). A similar equation can be derived to give a solution for κ_{1L}, and the beam position can then be calculated in the usual way (difference over sum) to give the horizontal position of beam 1.

CONCLUSION

The new BPMs in the ATLAS and CMS interaction regions must be able to accurately recover the individual position of each beam from a set of stripline signals that are sensitive to the position of both. The response of the BPMs to a beam stimulus was simulated in CST Microwave Studio and used to generate ensembles of waveforms that could be used to assess the performance of different compensation schemes. The initial simulations suggest a pulse-by-pulse approach is likely to deliver sufficient performance without requiring an unfeasible amount of digital processing.

Future studies will investigate the use of a pilot-tone scheme in order to compensate for differences in the behaviour of each channel.

REFERENCES

[1] CST Microwave Studio, http://www.cst.com

[2] M. Wendt, "BPM systems: A brief introduction to beam position monitoring", arXiv:2005.14081

[3] J. W. Eaton, D. Bateman, S. Hauberg, and R. Wehbring, "GNU Octave version 5.2.0 manual: a high-level interactive language for numerical computations", http://www.gnu.org/software/octave/doc/interpreter

[4] R. De Maria, S. D. Fartoukh, and M. Fitterer, "HLL-HCV1.1: optics version for the HL-LHC upgrade", in *Proc. 6th Int. Particle Accelerator Conf. (IPAC'15)*, Richmond, VA, USA, May 2015, pp. 2090–2093. doi:10.18429/JACoW-IPAC2015-TUPTY037

[5] M. Morgan, "Synthesis of a new class of reflectionless filter prototypes", arXiv:1008.3502